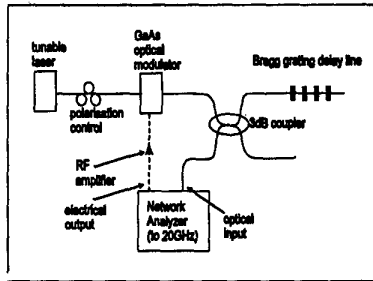


CWC5 Fig. 1 Time-delay measurement experimental arrangement for 1 GHz RF modulation frequency.

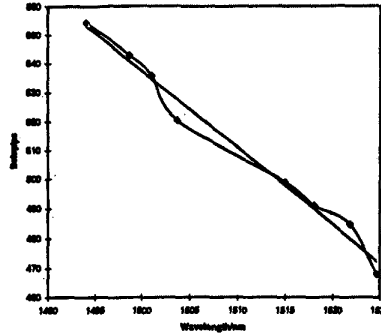


CWC5 Fig. 2 Time-delay measurement experimental arrangement for RF modulation frequency range 130 MHz-20 GHz.

ported here accesses the inherent advantage of wavelength-selected time delays through the use of a series of Bragg grating reflectors,³ of different central wavelengths, distributed along a single length of fiber.^{4,5} Individual gratings may be addressed by wavelength tuning the optical source, thereby changing the total length of fiber traversed by the optical signal, and so selecting the time delay.

In this paper we present the fabrication and measurement of the first three-bit optical fiber Bragg grating TTD delay line capable of producing time delays of the order of 10 ps. This delay line is suitable for beamforming control at RF frequencies up to ~2.8 GHz with 10° phase resolution. A fiber Bragg grating delay line, containing eight gratings, was fabricated in borongerminia codoped single-mode fiber, which had been presensitized by immersion in hydrogen.⁶ Each grating had a length of 2 mm, a FWHM bandwidth of ~0.5 nm, and a peak reflectivity of ~60%. The delay line was fabricated to have a 1-mm center-to-center spacing between the gratings.

The minimum achievable time delay was measured using two independent measurement systems, the first, shown in Fig. 1, operating at an RF modulation frequency of 1 GHz, and the second, shown in Fig. 2, operating over the RF frequency range 130 MHz-20 GHz. Light from a tunable laser was amplitude modulated



CWC5 Fig. 3 Absolute time delay as a function of wavelength; RF frequency range 130 MHz-20 GHz.

and coupled into the delay line via a 3-dB coupler, and the reflected light monitored by the vector voltmeter and network analyzer respectively. The phase of the reflected optical signal was compared to that of the RF modulation signal, thereby measuring any additional phase acquired by the optical signal, which was subsequently converted to the equivalent time delay using the following expression:

$$\Delta\theta = 2\pi\Delta T f$$

where $\Delta\theta$ is the phase delay acquired by the signal, ΔT is the equivalent time delay, and f is the RF modulation frequency.

The measured absolute time delay, at the peak reflection wavelength of each grating, was plotted as a function of wavelength (position along the delay line). The 130 MHz-20 GHz results are shown in Fig. 3; the gratings lie on a dispersion of -2.65 ps/nm, with a standard deviation of ± 0.15 ps/nm. The small deviations of the experimentally measured values away from the straight-line fit can be attributed to uncertainties in the precision of the positioning of the Bragg gratings during fabrication, and to resonance effects caused by the physical overlapping of the gratings, which are currently being investigated. To create significantly smaller time delays we envisage the use of broadly chirped Bragg gratings.⁷

*GEC-Marconi Materials Technology Limited, Caswell, Towcester, Northants, U.K., NN12 8EQ

1. W. S. Birkmayer, M. J. Wale, IEE Proc. Pt. J, 139, 301 (1992).
2. R. J. Mailloux, Proc. IEEE 70, 246 (1982).
3. G. Meltz, W. W. Morey, W. H. Glenn, Opt. Lett. 14, 823 (1989).
4. G. A. Ball, W. H. Glenn, W. W. Morey, IEEE Photon Technol. Lett. 6, 741 (1994).
5. A. Moloney, C. Edge, I. Bennion, Electron Lett. 31, 1485 (1995).
6. P. J. Lemaire, R. M. Atkins, V. Mizrahi, W. A. Reed, Electron. Lett. 29, 1191 (1993).
7. M. C. Farries, K. Sugden, D. C. J. Reid, I. Bennion, A. Molony, M. J. Goodwin, Electron. Lett., 30, 891 (1994).

CWC6

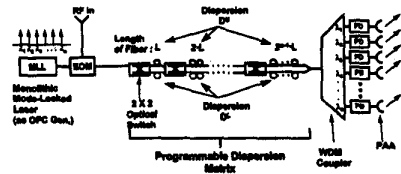
9:30 am

Programmable-dispersion matrix for optical beam-forming network

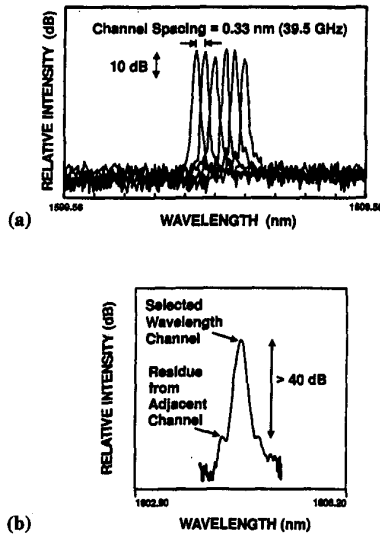
Dennis T. K. Tong, Ming C. Wu, UCLA, Electrical Engineering Department, Box 951594, Los Angeles, California 90095-1594

Dispersion of optical fiber is shown to reduce the complexity of optically controlled phased-array antenna (OCPAA) system.¹⁻³ For example, we have demonstrated a multiwavelength OCPAA system using only one mode-locked semiconductor laser and one single-mode dispersive fiber.² To further enhance the resolution of the antenna scan angle with limited number of optical wavelength channel, we demonstrate here a programmable-dispersion matrix (PDM) to be implemented in a multiwavelength OCPAA system. This PDM, when used in conjunction with optical-frequency comb generator, establishes a extremely hardware compressive system. Only one PDM and one optical comb generator are required to generate all the time delays for the entire array. In additions, the number of fiber lines needed in the PDM increases only logarithmically with the scan resolution.

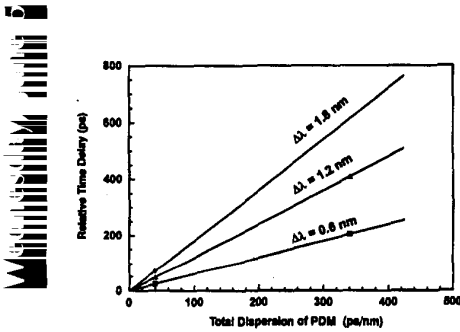
Figure 1 shows a PDM implemented for a n-bit resolution and m array elements antenna system. A monolithic mode-locked semiconductor laser is used as an optical-frequency comb generator. The mode-locked supermode provides m equally spaced wavelengths, $\lambda_1, \lambda_2, \dots, \lambda_m$ and each of these wavelengths is amplitude-modulated simultaneously by an external electro-optic modulator (EOM). Relative time delays among the optical wavelengths are introduced by the PDM. The processed wavelengths are sent to the antenna array through a WDM demultiplexer. Each array element is assigned an optical wavelength so that "wavelength channel-to-array element" correspondence is established. In order to extract each wavelength channel from the mode-locked supermode, a high-resolution spectrometer is needed. By using a double-grating filter, we have successfully extracted six wavelength channels from a 40-GHz monolithic colliding-pulse mode-locked semiconductor laser. More importantly, a side-mode suppression ratio of 40 dB is achieved, as shown in Fig. 2. Other filter³ such as a channel dropping filter or a fiber Fabry-Perot filter can also be used for the same purpose.



CWC6 Fig. 1 Schematic diagram of the multiwavelength OCPAA system using a programmable-dispersion matrix.



CWC6 Fig. 2 (a) Six wavelength channels extracted from a 40-GHz monolithic colliding-pulse mode-locked spectrum. (b) Single wavelength with side-mode suppression ratio of 40 dB is achieved for each channel.



CWC6 Fig. 3 Relative time delay among wavelength channels as a function of the total dispersion of the PDM.

In general, a n -bit resolution PDM can be constructed by using $n \times 2 \times 2$ optical switches and n pairs of fiber delay lines with different dispersion (e.g. D^u and D^l ps/nm-km) and lengths of $L, 2 \cdot L, \dots, 2^{n-1} \cdot L$, respectively. By controlling the $n \times 2 \times 2$ optical switches, the optical path through which the modulated signal travels can be programmed. The normalized dispersion of the optical path is

$$\mathcal{D} = D^u + \Delta D \cdot \sum_{i=0}^{n-1} \frac{2^i \cdot S_i}{2^i} \quad (1)$$

where $\Delta D = D^u - D^l$ and $S_i = 0$ or 1 , depending on the state of the $(i + 1)$ th optical switch. The resulting time delay introduced between adjacent wavelength channels is

$$\Delta T = \mathcal{D} \cdot (2^{n-1} - 1) \cdot L \cdot \Delta \lambda. \quad (2)$$

The WDM demultiplexer direct λ_i to the i -th element of the array, generating linear time shift of $\{0, \Delta T, 2 \times \Delta T, \dots,$

$(n - 1) \times \Delta T\}$ are generated across array elements.

To demonstrate the feasibility of this approach, Fig. 3 shows the measured relative time delay among optical wavelength as a function of the total dispersion of the PDM, using 80 GHz ($\Delta \lambda = 0.60$ nm) as the multiwavelength source. A relative time delay of 23.5 ps and 204 ps between adjacent optical channels are introduced for total dispersions of 39.1 and 340 ps/nm, respectively. The system can be made even more compact by using fiber grating as "taylorable" dispersive fiber. The concept of PDM also has applications in optical fiber networks for dispersion compensation.

In conclusion, we have demonstrated a programmable-dispersion matrix. This PDM, when implemented with a multiwavelength optical source in an OCPAA system, can generate all the time delay required for beam forming.

1. Esman, M. Y., Frankel, J. L. Dexter, L. Goldberg, M. G. Parent, D. Stilwell, D. G. Cooper, IEEE Photon. Technol. Lett. 5, 1347-1349 (1993).
2. Soref, Appl. Opt. 31, 7395-7397 (1992).
3. K. Tong, M. C. Wu, IEEE/LEOS 1995 Summer Topical Meeting, August 7-11, 1995, Keystone, Colorado, paper ThC4.

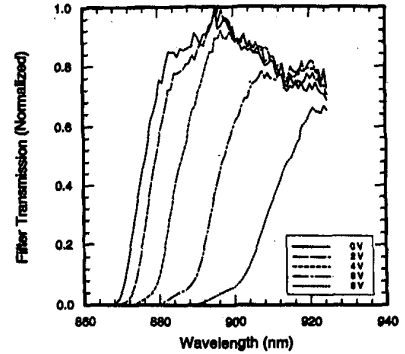
CWC7 9:45 am

Wavelength monitoring in fiber-optic sensors using a tunable optical waveguide filter

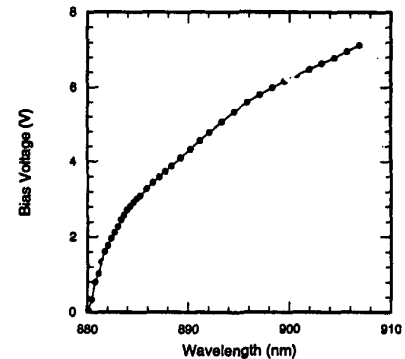
X. Wu, D. M. Bruce, P. E. Jessop, T. Coroy,* R. M. Measures,* Centre for Electrophotonic Materials and Devices, McMaster University, Hamilton, Ontario, Canada L8S 4L7

In sensor systems that are based on optical fiber Bragg gratings the center wavelength of the grating reflection must be determined with a precision on the order of hundredths of a nm over an operating range of several nm. Systems have been reported using interference filters,¹ long-pass transmission filters¹ and Mach-Zehnder interferometers² to provide the required wavelength discrimination. With these there is a trade-off to be made between the conflicting requirements of a large filtering slope (in %/nm) and a wide range of operating wavelengths. We report on the use of a GaAs/AlGaAs multiple quantum well³ optical waveguide modulator to serve as a sharp-edged filter that can be voltage tuned over several nm.

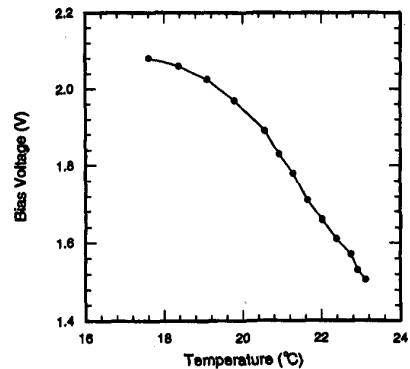
An optical fiber coupler is used to split the incoming light into a reference arm and a filtered arm. The latter is end-fire coupled to a 9.5-mm-long optical waveguide modulator. The reference signal and the light transmitted through the modulator are detected with silicon photodiodes resulting in a photocurrent ratio that is sensitive to wavelength and insensitive to the input intensity level. Figure 1 shows the observed ratio as a function of input wavelength for five values of the



CWC7 Fig. 1 Relative transmission through the optical waveguide modulator as a function of wavelength for five values of the bias voltage.



CWC7 Fig. 2 Wavelength dependence of the bias voltage that maintains a constant relative transmission through the modulator.



CWC7 Fig. 3 Variation of the locked bias voltage as a function of the modulator temperature for a wavelength of 882 nm.

reverse bias voltage applied to the p-i-n modulator. These data were taken using an attenuated titanium sapphire laser as the source.

In a wavelength range between 880 and 910 nm the sensitivity can be optimized by setting the bias voltage so that the photocurrent ratio is midway be-